High-definition transcranial direct current stimulation over the dorsal premotor cortex reliably modulates motor network excitability

Stephanie Lefebvre[1], Kay Jann[2], Allie Schmiesing[1], Kaori Ito[1], Mayank Jog[2], Yuchuan Qiao[3], Ryan Cabeen[3], Yonggang Shi[3], Nicolas Schweighofer[4], Danny JJ Wang[2], *Sook-Lei Liew[1]

1 Neural Plasticity and Neurorehabilitation Laboratory, University of Southern California, Los Angeles, CA United States,
2 Laboratory of FMRI Technology, USC Stevens Neuroimaging and Informatics Institute, Keck School of Medicine of USC, University of Southern California, Los Angeles, CA,
3 Laboratory of Neuro Imaging (LONI), USC Stevens Neuroimaging and Informatics Institute, Keck School of Medicine of USC, University of Southern California, Los Angeles, CA, USA.
4 Computational Neuro-Rehabilitation Laboratory, University of Southern California, Los Angeles, CA,

***Corresponding author**:

Sook-Lei Liew

sliew@chan.usc.edu

Title 15 words (max 15)

Abstract 148 words (max 150)

Main text:5581

Methods:2452

References: 70 (max 70)

Figures: 7

Tables: 1

Supplementary Methods: 1

Supplementary Data: 3

Supplementary Discussion: 1

Supplementary Figures: 3

Supplementary Table: 1

Abstract (149 words)

The effectiveness of transcranial direct current stimulation (tDCS) over the primary motor cortex (M1) to modulate motor network excitability is highly variable. The dorsal premotor cortex (PMd) may be a promising alternative target, as it provides high-level control of motor behavior using multiple pathways, including one independent of M1 and one with direct, influencing connections to M1. We differentially targeted these two close brain regions (M1, PMd) using a new high-definition tDCS (HD-tDCS) system with concurrent functional magnetic resonance imaging. PMd HD-tDCS led to more reliable changes in both cortical excitability and motor network complexity, measured by multiscale entropy, than M1 HD-tDCS or sham. PMd responsiveness was also positively correlated with the strength of the corticospinal tract from PMd. Additionally, this method revealed high anatomical variability in individual M1 and PMd localizations using canonical methods. Altogether, these results provide new considerations for improving tDCS effects on motor network modulation.

Transcranial direct current stimulation (tDCS) is a noninvasive tool that can modulate cortical excitability in human brain regions[1]. The effects of tDCS on upper limb motor rehabilitation have been widely studied, and more than 20 studies have shown promising effects of tDCS applied over the primary motor cortex (M1) on post-stroke motor recovery[2,3]. However, a major issue that prevents tDCS from being widely adopted in clinical practice is the high inter-individual variability shown in behavioral or cortical physiological[4,5] changes following M1 stimulation. The reasons for this inter-individual variability have not been fully elucidated (for a review, see Lefebvre & Liew, 2017[2]).

A potential solution to reduce the inter-individual variability is to use alternative stimulation sites and/or tDCS montages. That is, it is possible that stimulating another entry point into the motor network may lead to more reliable changes following tDCS. To date, the majority of tDCS studies for motor rehabilitation have focused on targeting M1 to alter motor network excitability based on two primary reasons. First, the site for M1 stimulation can be easily personalized to each individual using transcranial magnetic stimulation (TMS) to identify the individual's motor hotspot, which is assumed to represent M1. Second, since M1 is the primary region associated with descending motor pathways to the spinal cord (i.e., 50% of the corticospinal tract (CST) neurons originate in M1[6]), it makes sense to target this region to influence motor behavior. However, given the variable responses in stimulating M1, other stimulation sites that have functional connections with M1 should also be considered.

The dorsal premotor cortex (PMd) is a promising alternative neural target for modulating motor excitability. The PMd is the second major origin of the CST with 30% of CST projections[6,7]. As a higher motor area[8], the PMd contributes to motor control of the upper limb using a downstream pathway that is independent of M1[6,9,10], leading to some high-level control of motor commands[11].

Moreover, neural inputs to the hand and forelimb representation in M1 mostly originate from PMd[12,13], creating a cortico-cortical circuitry that has influences on motor network excitability[14-17]. Studies using monkeys have shown that if there are cortico-cortical connections between M1 and premotor cortex, the onset of the movement-related activity is always earlier in the premotor cortex. This suggests that these connections are initiated from the premotor cortex[11,18]. As such, PMd may modulate motor output in two ways: first, through its dedicated CST projections to the spinal cord; second, through its direct controlling connection to M1. Thus, due to its strong involvement in motor learning[19], motor selection, movement planning and preparation[9], and its controlling role over M1 excitability, PMd provides a promising alternative target for modulating motor network excitability. Stimulating PMd could also make the motor network more susceptible to cortical excitability changes. Only a few studies have examined the use of tDCS to modulate PMd, but most of them suggest that targeting PMd with tDCS could enhance motor performance and motor learning (for a review, see Buch et al., 2017[20]). However, to our knowledge, there are no studies directly comparing the effects of M1 and PMd-tDCS on motor network excitability.

This lack of direct comparison between M1 and PMd as targets for tDCS is likely due to a major drawback of conventional tDCS montages, which is their poor spatial resolution. The distribution of the electrical current using a standard tDCS montage is relatively diffuse, leading to changes far beyond the stimulated regions[21]. Therefore, trying to target M1 with conventional tDCS likely involves stimulation of at least a part of PMd[22]. The main reason for diffuse current densities in conventional tDCS montages is the large inter-electrode distance, which is limited by the size of the conventional electrodes (e.g., 5x5 or 5x7 cm). In contrast, recently introduced high-definition tDCS (HD-tDCS) devices provide the ability to increase stimulation focality[23] by delivering current through a 4x1 ring montage using smaller electrodes, making it possible to differentially target M1

and PMd. Although there is still likely a little overlap in the stimulation, the ring configuration helps to focus the peak stimulation over the targeted area.

We assessed changes in motor network excitability following M1 versus PMD tDCS using two primary methods: (1) changes in cortical physiology using TMS and (2) changes in motor network connectivity and complexity using resting-state fMRI (rs-fMRI). More specifically, TMS-induced motor evoked potentials (MEP)[1] were used to evaluate cortical excitability locally in the stimulated area, while rs-fMRI[24] was used to measure brain activity pre- and post-stimulation more broadly across the motor network. We used rs-fMRI to estimate functional connectivity (FC) of the motor network as well as to calculate multiscale entropy (MSE), which reflects the complexity of regional BOLD signals[25,26]. FC and MSE are complementary measures of network integrity, and MSE has been shown to reflect the dynamics of neural networks across multiple time scales or temporal frequencies[27]. Specificially, MSE changes during rs-fMRI have been reported following tDCS[25,28]. Since the complexity of neural activity fluctuations is associated with the probability of neural firing[26], this makes MSE a particularly relevant measure for assessing excitability changes following anodal tDCS, which is thought to increase the probability of neural firing[29].

The present study harnesses recent methodological innovations to examine concurrent HD-tDCS and fMRI. This technique provides the unique opportunity to not only explore whether stimulation of different areas in the motor network (M1 vs PMd) may have different effects on motor network cortical excitability but also to see if there were associated local or network changes underlying these effects, allowing us to more carefully examine mechanisms of plasticity. An additional benefit of this concurrent method is the ability to localize the stimulation electrodes on each individual's brain, to assess whether the stimulated region matched the targeted region.

Finally, using both functional and structural brain imaging, we were able to examine whether there were any neuroimaging predictors of response to HD-tDCS in any of the groups (M1, PMd, sham).

In this study, we hypothesized that stimulating the left PMd with HD-tDCS would modulate motor network excitability more reliably than stimulating left M1 in healthy individuals, due to the additional motor pathways emerging from PMd. We also examined whether there were concurrent changes in motor network connectivity and complexity related to tDCS responsiveness in each group using both standard functional connectivity and newer MSE approaches. We further explored whether there were any functional or structural neuroimaging predictors of HD-tDCS responsiveness in each group. Finally, we examined each individual's stimulated location in relation to the targeted stimulation locations to see whether interindividual variability in the stimulated location might relate to HD-tDCS responsiveness.

MATERIAL AND METHODS

Population

The protocol was approved by the University of Southern California Institutional Review Board. All subjects gave written informed consent in accordance with the 1964 Declaration of Helsinki. The inclusion criteria were the following: (1) being a healthy volunteer aged 18 – 50 years, (2) being right-handed. The exclusion criteria were the following: (1) having a pacemaker or other piece of metal in the body, (2) pregnancy, (3) previous history of stroke or other brain damage, (4) previous history or family history of epilepsy, (5) previous history of head injury, (6) previous history of skull damage, (7) previous history of migraines, (8) currently taking any medications that may affect cortical excitability (e.g. benzodiazepines), (9) inability to understand the instructions. Forty-six healthy participants took part in this double-blind, placebo-controlled study (neither the participants nor the primary experimenter knew the nature of the stimulation (e.g., real or sham HD-tDCS)). At inclusion, a first experimenter randomly assigned each participant into one of the following 3 groups: HD-tDCS applied over left M1, HD-tDCS applied over left PMd or sham HD-tDCS (in which case, electrodes were randomized over M1 or PMd). The second experimenter, who performed the data acquisition and analysis, was only aware of the location of the electrodes but remained blinded to whether participants received real or sham tDCS.

Study design

The study involved a single three-hour visit which included the following 3 sessions (see Figure 1): (1) a pre-MRI TMS session, including the localization of M1 and PMd as well as the recording of neurophysiological measurements, (2) a concurrent HD-tDCS/MRI session, including the placement of the HD-tDCS cap, acquisition of structural MRI sequences, a pre-HD-tDCS rs-fMRI scan, the double-blinded HD-tDCS stimulation with concurrent acquisition of rs-fMRI scan, as well

as a post-HD-tDCS rs-fMRI scan, and (3) a post-MRI TMS session to measure changes in neurophysiological measurements following HD-tDCS. To our knowledge, this is the first known randomized, group study using a concurrent HD-tDCS and fMRI paradigm in humans. The safety of these concurrent designs was established in a pilot study from Gbadeyan and collaborators in 2016 using both phantoms and a single participant[30]. They also examined the tolerability of their specific double ring HD-tDCS montage in a behavioral session (without fMRI) in 30 participants.

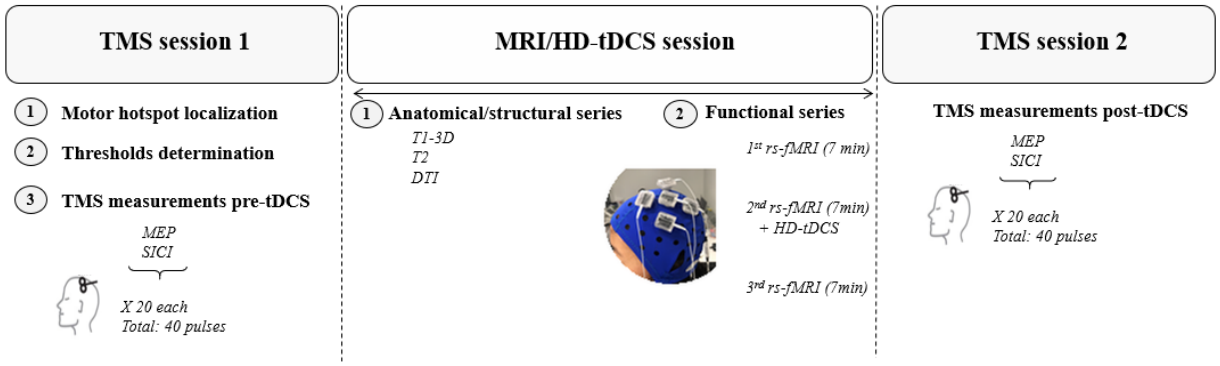

Figure 1: Study design. Each participant will take place in 3 sessions as follows: a first TMS session, then an MRI/HD-tDCS session, and finally a second TMS session. *HD-tDCS: high-definition transcranial direct current stimulation, MEP: Motor Evoked Potential, RMT: Resting Motor Threshold, rs-fMRI: resting-state functional magnetic resonance imaging.*

<u>Pre-MRI TMS session</u>

Briefly, we used single- and paired-pulse transcranial magnetic stimulation (TMS) (Magstim 200² device with BiStim module; Magstim Inc., UK) with a figure-of-eight coil, along with the Brainsight neuronavigation system (Rogue Resolutions Ltd, UK) and surface electrodes to record muscle activity (electromyography, or EMG; Delsys Trigno wireless sensors, Delsys Inc, MA). To localize the motor hotspot, we recorded EMG at the right first dorsal interosseous (FDI). We then recorded pre-HD-tDCS cortical excitability, including each individual's resting motor threshold (RMT) and single-pulse motor-evoked potentials (MEPs) with a test stimulus at the intensity

needed to generate an MEP of 0.75mV peak-to-peak amplitude. Notably, this test stimulus is in accordance with previous studies showing a range of test stimuli between 0.2mV and 4mV[31,32]. We also measured short-interval intracortical inhibition (SICI) using a paired-pulse TMS paradigm (see Brain Stimulation Intervention section below for details on the TMS paradigms). MEPs were recording using Signal 6.05 software (Cambridge Electronic Design Ltd., UK).

MRI session

Immediately following the first TMS session, participants were fitted with the HD-tDCS cap and began an MRI session including the acquisition of an anatomical image (T1w MPRAGE), a T2-weighted anatomical MRI, a diffusion-weighted MRI, a 7-minute baseline rs-fMRI (pre-HD-tDCS rs-fMRI), a second 7-minute rs-fMRI during which participants received sham or HD-tDCS applied over M1 or PMd, depending on their group, and a third 7-minute rs-fMRI to assess the after effects of HD-tDCS (see MRI section below for more details). An additional experimenter, who was unblinded to the stimulation condition (real or sham), turned the tDCS stimulation device on and off. In this way, the primary experimenter and participant remained blinded to the stimulation condition.

Post-MRI TMS session

Immediately following the MRI session, the participants took part in a second TMS session to quantify the HD-tDCS-induced changes on cortical excitability. The cortical excitability measurements of this second TMS session started less than 10 minutes after the end of the third resting state fMRI scan (i.e., time for the participant to leave the MRI, walk to the adjacent TMS experimental room and have the HD-tDCS equipment removed and the TMS coil repositioned on their M1 hotspot).

Brain stimulation intervention

TMS paradigm

We defined the motor hotspot as the spot at which the maximal MEP peak-to-peak amplitude was recorded in the FDI muscle using a single TMS pulse at 50% ± 5% of the maximum stimulator output. We defined the RMT as the intensity of the stimulator that induced an MEP of at least 50 μV peak-to-peak amplitude in 5 out of 10 trials. We defined the test stimulus for the current study as the intensity of the stimulator that induced an MEP of at least 0.75mV ($TS_{0.75mV}$) peak-to-peak amplitude in 5 out of 10 trials.

After defining these thresholds, we used them in an MEP-SICI paradigm which consisted of 40 trials in a randomized order with a 7s ± 10% inter-trial duration. This paradigm included 20 single-pulse trials using the $TS_{0.75mV}$ (the peak-to-peak amplitude of these trials will be referred to as MEPs), and 20 paired-pulse trials using a conditioning stimulus (CT) at 80% of the RMT 2.5ms before the $TS_{0.75mV}$ (the peak-to-peak amplitude of these trials will be referred to as MEPs in SICI trials). We anticipated that the SICI trials should result in a decrease of the MEPs in SICI trials compared to MEP trials. Therefore, to analyze HD-tDCS effects on intracortical inhibition, we compared the ratio of the MEPs divided by the MEPs in SICI trials between pre and post-HD-tDCS. (For SICI results, see *Supplementary Data 1*).

For 6 participants (2 in each group), we were unable to reach the intensity needed to elicit a MEP of 0.75mV, or even 0.5mV. In these cases, we used the RMT as the test stimulus to acquire the MEPs. For one additional participant in the M1 group, we were only able to localize the motor hotspot but did not acquire any other neurophysiological measurements due to the participant's reported discomfort. This participant was included only in the resting-state analyses.

HD-tDCS experiment

We used the Soterix MRI-compatible HD-tDCS system (4x1 ring configuration) to deliver tDCS (1mA) for 7 minutes during an fMRI session (see Figure 1). We used 5 small gel-filled electrodes (base diameter: 2.4 cm, gel-skin contact area of ~4.5 cm^2) positioned in adjacent electrode locations within the cap, and we placed the center electrode on the cap over the location of the neural target (as defined below). Each of the 4 cathodal ring electrodes delivered a -0.25mA current leading to a 1mA stimulation over the center anodal electrode.

Localization of the HD-tDCS targets

For the M1 group, we positioned the center electrode over the motor hotspot, and for the PMd group, we positioned the center electrode 2.5cm anterior to the motor hotspot, which is the standard localization for PMd[33]. The use of this MRI-compatible device also gave us the unique opportunity to obtain an anatomical MRI with the exact position of the electrodes on the participant's own head. We therefore also report the localization of individual stimulation sites across participants in the Results section.

MRI session acquisition and preprocessing

MRI acquisition

MRI data were acquired on a 3T Prisma MRI scanner (Siemens, Germany) with a 32-channel head coil using protocols from the Human Connectome Project (HCP) (*http://protocols.humanconnectome.org/CCF/;https://www.humanconnectome.org/storage/app/media/documentation/lifespan-pilot/LSCMRR_3T_printout_2014.08.15.pdf)*. The MRI sequences acquired included the following: T1-weighted MPRAGE scan (208 sagittal slices, 0.8mm thick, TR = 2400ms, TE = 2.22ms, flip angle = 8°, voxel size 0.8 x 0.8 x 0.8mm); T2-weighted turbo spin-echo scan (208 sagittal slices, 0.8mm thick, TR = 3200ms, TE = 523ms, flip angle = 8°, voxel

size 0.8 x 0.8 x 0.8mm); diffusion MRI scan (92 slices, 1.5 mm thick, TR = 3230ms, TE = 89.20ms, multi-band factor = 4, flip angle = 78°, voxel size 1.5 x 1.5 x1.5mm, with a gradient protocol with 7 scans at b=0 s/mm2, 47 at b=1500 s/mm2, 46 at b=3000 s/mm2, and a complete repetition with reversed phase encoding in the A-P direction); and three rs-fMRI sequences (7 minutes and 6 seconds covering 520 volumes of 72 slices per scan; TR = 800ms, TE = 37ms, flip angle = 52°, voxel size 2 x 2 x 2mm).

Resting-state fMRI processing

We analyzed the rs-fMRI data using SPM12, the CONN toolbox (FC toolbox[34]; http://www.nitrc.org/projects/conn) and the Complexity Toolbox (http://loft-lab.org/index-5.html). The preprocessing steps included slice-timing correction, motion realignment, noise correction using white matter, CSF and motion parameters as regressors, and band-pass filtering (0.01-0.1 Hz). We also performed co-registration between the functional scans and 3D-T1w MPRAGE scans of each participant. Finally, we normalized the functional scans to MNI space and smoothed them using a Gaussian filter of 6mm.

To measure functional changes in the motor network, we compared the FC between regions of interest (ROI-to-ROI analyses) and analyzed the neural complexity by computing the MSE of the BOLD time series in each ROI (defined below) before and after HD-tDCS.

ROI-to-ROI analyses

We defined 4 ROIs as the left M1, right M1, left PMd and right PMd. We used a meta-analysis from Hardwick and collaborators[19] to define the localization of the ROIs in the left hemisphere and then flipped them to the right hemisphere. The exact coordinates of the center of each ROI, which was defined as a sphere with a radius of 10mm, were: left M1 (x = -38, y = -24, z = 56), right M1 (x = 38, y = -24, z = 56), left PMd (x = -26, y = 2, z = 60), right PMd (x = 26, y = 2, z = 60).

In addition, as an exploratory analysis, we also defined an additional ROI to represent the whole motor network, which was defined from a spatial map from an independent component analysis (ICA) on the rs-fMRI data before HD-tDCS was administered (Figure 2). Although we primarily use the main 4 Hardwick ROIs (left and right M1 and PMd) for most analyses, when analyzing the difference between each ROI and the whole network, we use this ROI as the definition of the whole network. Additional methods on the ICA analysis are presented in *Supplementary Methods 1*.

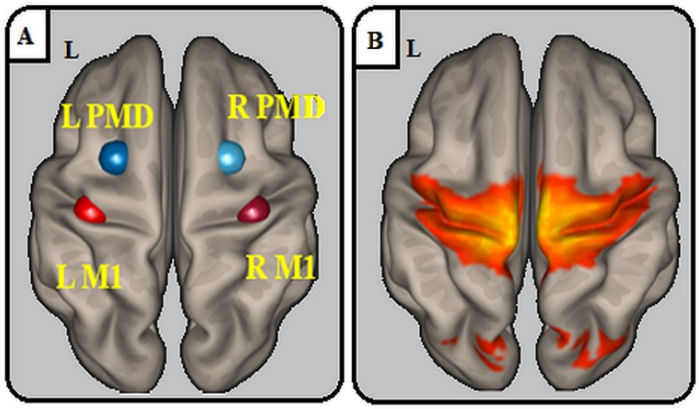

Figure 2: Localization of the regions of interest. Panel A: Localization of the 4 ROIs based on the meta-analysis from Hardwick and collaborators[19]. Each ROI was defined as a sphere with a radius of 10mm around the reported peak coordinates for each region. These were: left M1 (x = -38, y = -24, z = 56), right M1 (x = 38, y = -24, z = 56), left PMd (x = -26, y = 2, z = 60), right PMd (x = 26, y = 2, z = 60). Panel B: The whole motor network component as generated from the pre-HD-tDCS spatial map from the ICA analysis. *L: left, M1: primary motor area, PMd: dorsal premotor cortex, R: right, ROI: region of interest*

We extracted the cross-correlations of these 4 ROIs (left/right M1, left/right PMd) and ordered them for each group and each condition based on the correlation intensity. To compare the organization of the motor network following each stimulation session, we compared these orders using Spearman's rank correlations coefficient.

We also used RM-ANOVAs (one RM-ANOVA for each ROI as a seed region) in the CONN toolbox to compare combinations of pairs between the 4 ROIs (the 6 FC pairs were: left M1-right

M1, left PMd-right PMd, left M1-left PMd, left M1-right PMd, left PMd-right M1, right M1-right PMd) using "Time" (pre-HD-tDCS, post-HD-tDCS) and "Group" (M1, PMd and sham) as factors.

Multiscale-entropy

MSE was used to evaluate changes in neural complexity following HD-tDCS in each of the 4 ROIs (left M1, right M1, left PMd, right PMd). The MSE metric quantifies the regularity or complexity of biological signals across a range of coarse-grained time scales or temporal frequencies. Complex systems with $1/f$ power spectra exhibit constant entropy over various time scales (due to their fractal properties), whereas random noise shows a marked decrease in entropy at longer time scales (as random fluctuations are smoothed out)[26]. We used a pattern matching threshold (r) of 0.5 and a pattern length (m) of 2[26,35,36]. In total, we obtained 20 coarse-sampled scales. Based on the band-pass filter applied, we kept only 9 scales for the analyses (scales 12 to 20).

Structural Correlates of MRI Responsiveness

In addition to measuring HD-tDCS-induced changes in rs-fMRI (connectivity and complexity), we also performed additional analyses to check for any potential anatomical factors that could explain or predict HD-tDCS-induced effects. Therefore, we also measured the strength of the corticospinal tract (using diffusion MR tractography) and the cortical thickness of the ROIs to see if any of these measures influence HD-tDCS effects.

Diffusion MRI

For the diffusion MRI preprocessing, we followed the HCP processing pipeline (*https://github.com/Washington-University/HCPpipelines/tree/master/DiffusionPreprocessing*). Then, we modeled each voxel with a multi-compartment fiber orientation distribution (FOD)

approach[37]. Finally, we obtained the diffusion tensor fractional anisotropy (FA) values using FSL and completed the deterministic FOD fiber tracking[38] using the Quantitative Imaging Toolkit (QIT)[39]. For each participant, we created three tracts: a global corticospinal tract (CST) in the left hemisphere, a CST section that originated from the left M1 and a CST section that originated from the left PMd (see Figure 3 for an example in one participant). For each participant, we first drew the global left CST from an ROI covering the left posterior limb of the internal capsule. Following this, we created two different sub-tracts by defining the overlap between the individual's global CST with M1 and PMd template tracts based on 100 subjects, as defined in Archer et al., 2018[40]. This resulted in a total CST tract, an M1 tract, and a PMd tract for each individual.

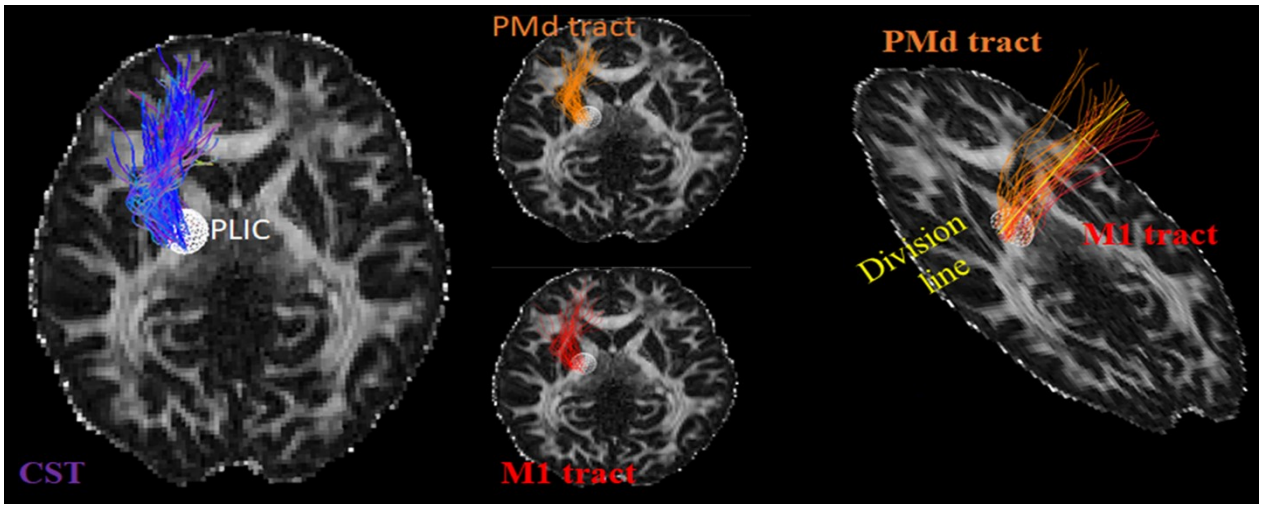

Figure 3: Example of the DTI tracts in one participant. Left panel: After positioning the PLIC ROI, we extracted the CST of the participant. Middle panel: By overlapping the CST obtained and the M1 or PMd template tract, we obtained the M1 and PMd tract for each participant. Right panel: Superposition of the M1 and PMd tracts for one participant. Note that the M1 tract is localized at the posterior part of the CST whereas the PMd tract is more anterior. The yellow division line is shown to visualize the separation between the two tracts. *PLIC: posterior limb of the internal capsule, CST: corticospinal tract, M1: primary motor area, PMd: dorsal premotor cortex*

Cortical thickness analysis

We used FreeSurfer software version 6 (*http://surfer.nmr.mgh.harvard.edu*) to automatically create a 3D model of the cortical surface for cortical thickness measurements on the T1-3D scans of all our participants[41]. We manually inspected the individual surfaces for potential segmentation errors between gray and white matter, and we manually corrected segmentations as needed. We computed cortical thickness measurements on each of the 4 ROIs (left M1, right M1, left PMd and right PMd) for each participant.

Statistical analyses

We used R (*https://www.r-project.org/about.html*) to perform all the statistical analyses, except for the analyses performed using the CONN toolbox (rs-fMRI FC). We used the CONN toolbox for ROI-to-ROI analysis, and the results are presented at a qFalse discovery rate = 0.05 (corrected for multiple comparisons).

We performed a repeated measures RM-ANOVAs to compare changes in MEPs across groups, and separate RM-ANOVAS to compare changes in MSE for each of the 4 motor ROIs. We used factors of "Time" (pre-HD-tDCS, post-HD-tDCS) and "Group" (M1, PMd and sham) in all RM-ANOVAs. To evaluate HD-tDCS-induced changes within each group, we also performed a priori analyses of pre/post HD-tDCS differences in MEPs for each of the 3 groups using two-way paired t-tests. We report the test statistics and p-values, along with the effect size, using partial eta squared (η_p^2) for the ANOVA main effects, and Cohen's d for the t-tests. Any post-hoc tests are corrected for multiple comparisons using the Tukey HSD.

To determine which parameters might influence the HD-tDCS effects, we estimated Pearson's correlation coefficients relating pre-HD-tDCS measurements (rs-fMRI FC, MSE, FA, cortical thickness) with the MEP changes in each of the M1 and PMd groups. We reported correlation p-

values that are both uncorrected (p_{uncorr}) and corrected for multiple comparisons (p_{corr}) using the Bonferroni correction for the 4 comparisons (rs-fMRI FC, MSE, FA, cortical thickness). Finally, we performed two-way independent samples t-tests to compare each of these 4 measurements between responders and non-responders. For the t-tests, we also reported both p_{uncorr} and p_{corr}. We defined the "responders" subgroup as participants in the M1 or PMd group who showed an increase in MEPs following HD-tDCS [(averaged MEPs' amplitude over the 20 trials post-tDCS) / (averaged MEPs' amplitude over the 20 trials pre-tDCS) > 1)]. The "non-responders" subgroup refers to participants in the M1 or PMd group who demonstrated a decrease or no change in MEPs following HD-tDCS [(averaged MEPs' amplitude over the 20 trials post-tDCS) / (averaged MEPs' amplitude over the 20 trials pre-tDCS) ≤ 1)]. Although there is a fine boundary between the two, we note that it has been consistently used to define responders/non-responders in the literature[5,42].

RESULTS

Neurophysiological measurements

Baseline thresholds

We first checked to see whether the initial cortical excitability between the 3 groups was similar by comparing the pre-HD-tDCS RMT and TS0.75mV across groups (Table 1).

Using two separate one-way ANOVAs with "Group" (M1, PMd, sham) as a factor, we found that there was no significant difference between the 3 groups for either the RMT (n = 45, Group effect: F(2) = 0.50, P = 0.61), or for the TS0.75mV threshold (n = 39, Group effect: F(2) = 0.49, p = 0.62).

Subject	Group	RMT	TS0.75mV	MEP pre-tDCS (mV)	MEP post-tDCS (mV)
s01	M1	48	55	1.14	2.37
s02	M1	--	--	--	--
s03	M1	47	65	1.72	0.87
s04	M1	47	55	1.33	1.68
s05	M1	50	57	2.22	1.78
s06	M1	50	69	1.17	0.96
s07	M1	41	47	0.86	0.46
s08	M1	43	70	0.94	2.25
s09	M1	46	54	0.79	0.24
s10	M1	59	--	0.07	0.07
*s11**	*M1*	*38*	*48*	*1.06*	*6.8*
s12	M1	47	--	0.18	0.15
s13	M1	58	75	1.64	1.92
s14	M1	46	66	0.91	1.63
s15	M1	37	64	0.95	1.39
Mean		*46.93*	*60.42*	*1.07 (*1.07)*	*1.21(*1.61)*
SD		*6.32*	*8.99*	*0.58 (*0.56)*	*0.80(*1.68)*
s16	PMd	38	57	1.18	3.26
s17	PMd	45	80	0.48	0.71
s18	PMd	50	63	0.38	0.43
s19	PMd	42	51	1.48	0.92
s20	PMd	44	53	0.98	2.56
s21	PMd	48	72	0.38	0.99
s22	PMd	38	44	1.17	2.32
s23	PMd	63	73	0.3	0.36

s24	PMd	54	--	0.11	0.43
s25	PMd	35	52	1.02	1.52
s26	PMd	51	--	0.21	0.08
s27	PMd	41	80	0.39	2.13
s28	PMd	38	39	0.52	0.25
s29	PMd	37	41	0.7	0.61
s30	PMd	39	56	0.49	1.38
Mean		*44.20*	*58.54*	*0.68*	*1.20*
SD		*7.74*	*14.06*	*0.41*	*0.97*
s31	sham	60	78	1.39	0.68
s32	sham	50	--	0.26	0.65
s33	sham	40	50	2.14	0.62
s34	sham	33	44	0.99	0.82
s35	sham	48	60	0.61	0.23
s36	sham	35	40	2.41	1.33
s37	sham	49	53	0.92	3.37
s38	sham	43	52	0.58	1.2
s39	sham	48	72	0.85	0.85
s40	sham	48	54	0.59	0.49
s41	sham	56	72	1.33	0.83
s42	sham	65	--	0.14	0.03
s43	sham	48	55	1.24	1.08
s44	sham	44	65	3.32	0.53
s45	sham	38	50	0.56	2.03
s46	sham	36	36	1.1	2.06
Mean		*46.31*	*55.79*	*1.15*	*1.05*
SD		*8.94*	*12.39*	*0.84*	*0.83*

Table 1: Initial cortical excitability measurements. *SD: standard deviation; RMT: resting motor threshold, *outlier, -- indicates the measurement could not be elicited. For the M1 group, MEP mean and SD are presented excluding the outlier and with the outlier (*).*

Changes in MEPs

Inter-individual variability in HD-tDCS response

We then assessed inter-individual variability in response to HD-tDCS between the 3 groups, focusing on the number of individuals showing changes in MEP following HD-tDCS in each group. We found considerable inter-individual variability in MEP changes following HD-tDCS in the 3 groups (Figure 4). In the M1 group, 7 out of 14 (50%) participants showed an increase in MEPs,

while in the PMd group, 11 out of 15 participants (73.3%) showed an increase in MEPs. Importantly, in the sham group, 6 out of 16 participants (31.25%) showed an increase in MEPs following sham HD-tDCS, suggesting that some individuals will show some level of change in cortical excitability without stimulation. The number of participants with increased MEPs post-HD-tDCS showed a trending difference across the 3 groups ($\chi^2(2) = 5.497$, $P = 0.06$). Due to the large variability, especially in the M1 group, we ran an outlier detection analysis, using the Quantile Range Outliers method to identify any outliers beyond 3 interquartile ranges (calculated on MEP amplitude across the entire cohort). In doing so, we identified and removed one participant with an outlier response in the M1 group from further excitability analyses (an increase in MEP amplitude following HD-tDCS of more than 3 interquartile ranges, or 4.2mV; see Figure 4).

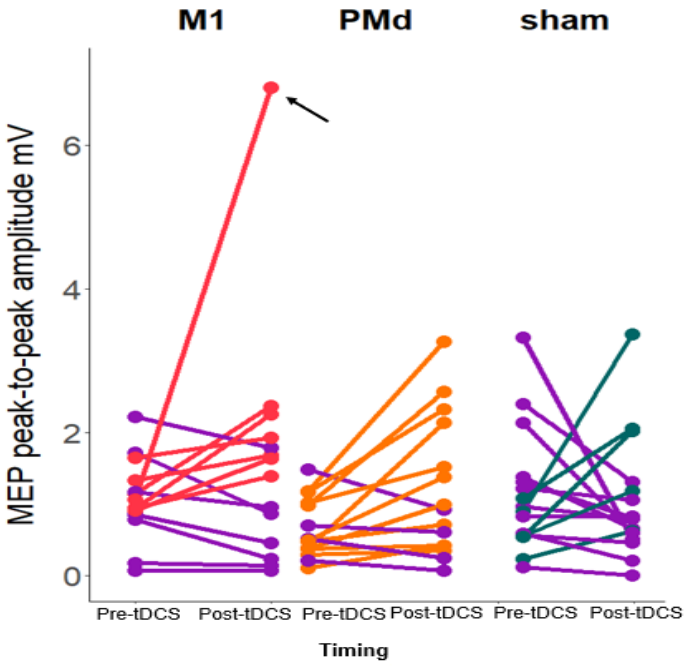

Figure 4: Individual changes in MEPs over time. The dot pairs reflect the MEPs pre and post-tDCS for each participant in each of the 3 groups. Participants who showed a decrease in MEP between pre and post-tDCS are displayed in purple. *In the M1 group, one participant presented a very strong effect post-tDCS. After running an outlier detection, this participant was removed from the rest of the analyses (indicated by the black arrow). *M1: primary motor area, MEP: motor evoked potential, mV: millivolts, PMd: dorsal premotor cortex, tDCS: transcranial direct current stimulation.*

Group level changes in MEPs

We next evaluated the magnitude of HD-tDCS-induced changes in cortical excitability across the 3 groups by comparing the amplitude of MEPs before and after HD-tDCS (Table 1, Figure 5).

A two-way RM-ANOVA was performed on the MEPs, with "Time" (pre-HD-tDCS, post-HD-tDCS) and "Group" (M1, PMd and sham) as factors. There were no significant interaction or group effects (RM-ANOVA: n = 44, Interaction Group*Time $F(2,41) = 1.88$, $P = 0.17$, $\eta_p^2 = 0.31$; Group: $F(2,41) = 0.52$, $P = 0.59$, $\eta_p^2 = 0.04$; Time: $F(1,41) = 1.83$, $P = 0.18$, $\eta_p^2 = 0.0030$). We then examined a priori comparisons of pre versus post HD-tDCS for each group. This demonstrated a significant increase in MEP amplitude only following PMd HD-tDCS (*PMd post > pre-HD-tDCS t(41) = 2.56, P = 0.03, Cohen's d = 0.73, M1 post > pre-HD-tDCS t(41) = 0.55, P = 0.58, Cohen's d = 0.20, sham post > pre-HD-tDCS t(41) = 0.44, P = 0. 66, Cohen's d = 0.12)*.

Finally, we examined whether there was a difference in the magnitude of MEP changes within the individuals who responded to M1 HD-tDCS versus PMd HD-tDCS. That is, even though more individuals showed an increased MEP following HD-tDCS in the PMd group than the M1 group, we wanted to evaluate whether the amplitude of the MEP changes was different between these two groups. Using just responders from M1 (n=6) and PMd (n=11) groups, a two-way RM-ANOVA with "Time" (pre-tDCS, post-tDCS) and "Group" (M1, PMd) as factors showed an increase in cortical excitability following HD-tDCS (RM-ANOVA: n = 17, Interaction Group*Time $F(1,27) = 0.13$, $P = 0.72$, $\eta_p^2=0.002$; Group: $F(1,15) = 2.74$, $P = 0.12$, $\eta_p^2 =0.12$; Time: $F(1,15) = 26.72$, $P = 0.0001$, $\eta_p^2=0.30$; post-hoc tests: *PMd post > pre-HD-tDCS* $t(15) = 4.37$, $P = 0.0005$, Cohen's d=1.12*, M1 post > M1 pre-HD-tDCS* $t(15) = 2.72$, $P = 0.014$*, Cohen's d=2.14, PMd pre >M1 pre-HD-tDCS t(42)=-1.61, P =0.13, Cohen's d=1.48).* This demonstrated that, when individuals

responded to HD-tDCS, there were no significant differences in MEP amplitude between M1 and PMd response.

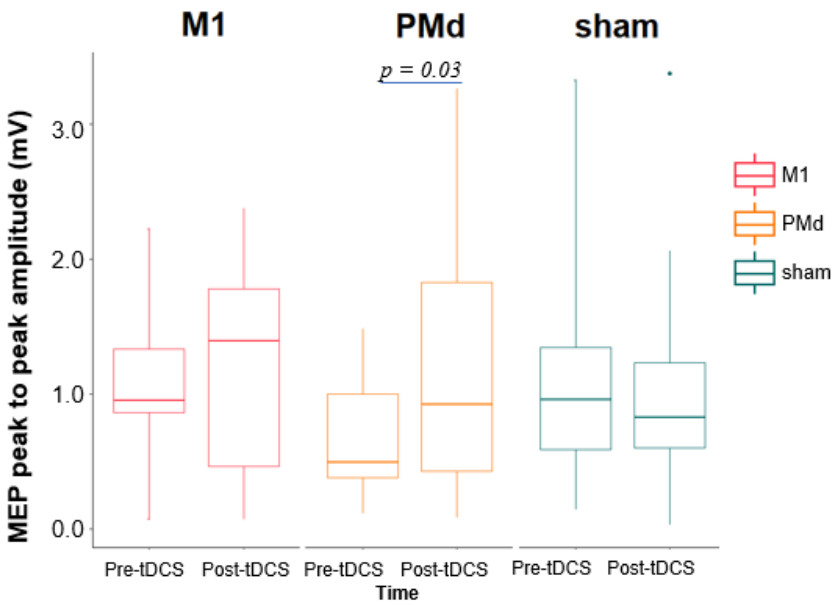

Figure 5: Changes in MEPs across groups. Box-and-whisker plots of the MEPs per group over time (pre/post-tDCS). The center line represents the median value, the lower bound of the box represents the 25th percentile, the upper bound of the box the 75th percentile, and the whiskers represent 3 times the interquartile range. Any outliers are indicated by dots. Note that the only statistically significant difference is observed in the PMd group reflecting an increase of the MEPs amplitude post-tDCS. *M1: primary motor area, MEP: motor evoked potential, mV: millivolts; PMd: dorsal premotor cortex, tDCS: transcranial direct current stimulation.*

Resting-state fMRI

Resting-state functional connectivity

We then examined whether there were overall changes in the functional organization of the motor network by comparing cross-correlation rankings for each of the ROI-to ROI pairs before versus after HD-tDCS. However, the global organization of the motor network did not change after HD-tDCS in any of the groups, as demonstrated by a strong rank correlation within each group between pre and post-HD-tDCS measurements (M1 group: n = 15, r = 0.88, $P = 0.03$, PMd group:

n = 15, r = 0.88, P = 0.03, sham group: n = 16, r = 0.94, P = 0.02). In addition, we compared changes in rank correlations between groups using a Fisher's Z test[43], which also showed no significant differences in correlation ranks between groups (M1 > PMd: z = 0.0, P = 1; M1 > sham: z = 0.78, P = 0.43, PMd > sham: z = 0.78, P = 0.43). This suggests that there was no global reorganization of the relative ROI-to-ROI connectivity strengths in the motor network following either M1 or PMd HD-tDCS.

We then examined changes in connectivity for each ROI-to-ROI pair using an ANOVA with Time and Group as factors (n = 46, thresholded at qFDR = 0.05; CONN toolbox). Here we also found no significant changes post-HD-tDCS in any of the 3 groups.

Using left PMd as the seed ROI, there were no significant changes in FC post-HD-tDCS in the M1 group (F(3,41) = 1.47, P = 0.67), the PMd group (F(3,41) = 0.18, P = 0.91) and the sham group (F(3,41) = 0.34, P = 0.94). Using right PMd as the seed ROI, there were no significant changes in FC post-HD-tDCS in the M1 group (F(3,41) =1.16, P = 0.67), the PMd group (F(3,41) = 0.18, P = 0.91) and the sham group (F(3,41) = 0.21, P = 0.94). Using left M1 as the seed ROI, there were no significant changes in FC post-HD-tDCS in the M1 group (F(3,41) = 0.55, P = 0.73), the PMd group (F(3,41) = 0.23, P = 0.91) and the sham group (F(3,41) = 0.33, P = 0.94). Using right M1 as the seed ROI, there were no significant changes in FC post-HD-tDCS in the M1 group (F(3,41) = 0.43, P = 0.73), the PMd group (F(3,41) = 0.39, P = 0.91) and the sham group (F(3,41) = 0.13, P = 0.94)

Additional exploratory analyses focusing on ROI-to-ROI comparisons and ICA network comparisons at a less stringent threshold (cluster-level corrected p<0.01) are reported in *Supplementary Data 2 & 3, Supplementary Figures 1 & 2, Supplementary Table 1, and Supplementary Discussion*.

Multi-scale entropy of resting-state fMRI

We then examined HD-tDCS-associated changes in MSE to examine potential changes of motor network excitability (Figure 6).

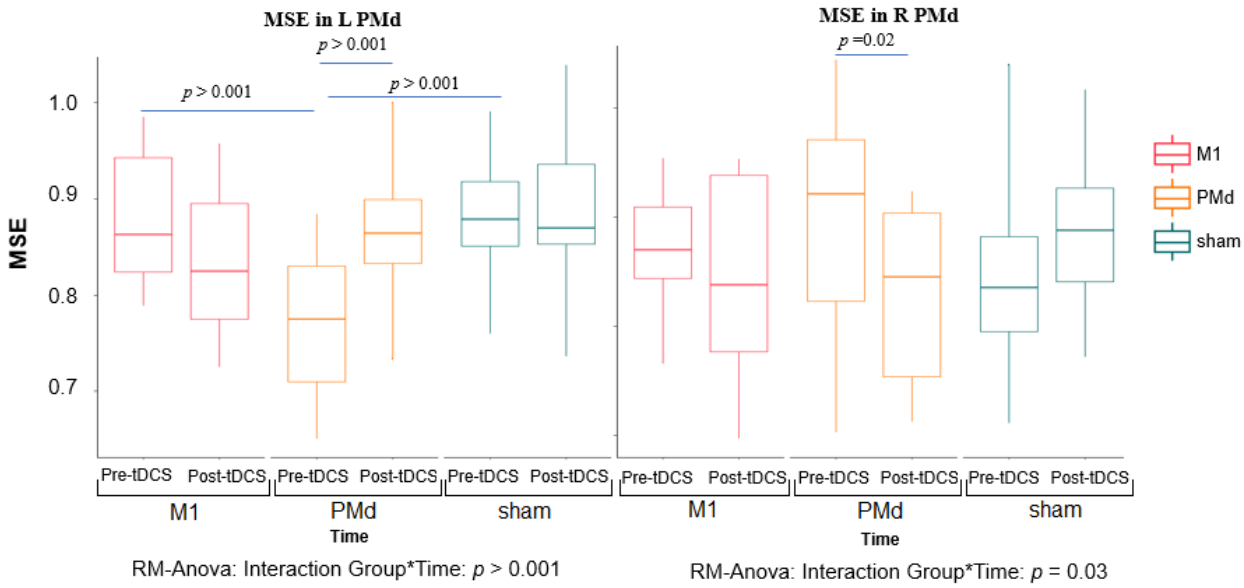

Figure 6: Changes in MSE across groups. Box-and-whisker plots of the MSE per group over time (pre/post-tDCS) in the left PMd ROI (in the left panel) and in the right PMd ROI (in the right panel). The center line represents the median value, the lower bound of the box represents the 25th percentile, the upper bound of the box the 75th percentile, and the whiskers represent 3 times the interquartile range. Any outliers are indicated by dots. *L: left, M1: primary motor area, MSE: multiscale entropy, PMd: dorsal premotor cortex, R: right, tDCS: transcranial direct current stimulation.*

RM-ANOVAs with "Time" (pre-HD-tDCS, post-HD-tDCS) and "Group" (M1, PMd, sham) as factors were performed for each of the 4 regions of interest (left/right M1, left/right PMd) and demonstrated a significant interaction between group and time and significant main effect of group, with a significant increase in MSE only in the left PMd following PMd HD-tDCS (Left PMd RM-ANOVA: n = 46, Interaction Group*Time F(2,43) = 9.06, $P = 0.0005$, $\eta_p^2 = 0.14$; Group: F(2,43) = 7.5 $P = 0.002$, η_p^2 0.19; Time: F(1,43) = 2.33, $P = 0.13$, $\eta_p^2 = 0.02$; post-hoc tests: *PMd post > pre-HD-tDCS* t(43) =4.09, $P = 0.0002$, Cohen's d=1.31, *M1 post > pre-HD-tDCS t(43) =-1.94, P*

= 0.06, Cohen's d=-0.61, sham post > pre-HD-tDCS t(43) = 0.50, P = 0.61, Cohen's d= 0.17). There was also a trend towards a decrease in MSE in the left PMd following M1 stimulation, but this was not significant.

There was also a significant interaction and main effect of group, with a decrease in MSE only in the PMd group in the right PMd after HD-tDCS (Right PMd RM-ANOVA: n = 46, Interaction Group*Time F(2,43) =3.89, *P = 0*.03, η_p^2= 0.09; Group: F(2,43) = 0.02, *P = 0*.9, η_p^2 = 0.0003; Time: F(1,43) =1.14, *P = 0*.29, η_p^2= 0.009; post-hoc tests: *PMd post > pre-HD-tDCS* t(43) =-2.43, *P = 0*.02, Cohen's d =-0.78*, M1 post > pre-HD-tDCS t(43) =-0.71, P = 0.48, Cohen's d=-0.28, sham post > pre-HD-tDCS t(43) =1.48, P = 0.14, Cohen's d= 0.60.* There were no significant findings in either left or right M1, and there were no significant correlations between changes in MSE with changes in MEPs in either the M1 or PMd groups.

Correlation between MEP changes and baseline functional/structural brain measures

We next calculated correlations between the changes in MEPs after HD-tDCS in M1 and PMd groups with a number of baseline functional connectivity and neuroanatomical measures to determine if any initial functional or structural measurements were predictive of changes in cortical excitability following HD-tDCS. Specifically, we assessed correlations between MEP changes and the following factors: (1) baseline rs-fMRI FC between M1/PMd and the whole motor network ROI, (2) the initial MSE complexity levels in M1/PMd, (3) the strength of the CST originating from M1 or PMd (as measured by fractional anisotropy), and (4) the cortical thickness in the M1/PMd. As a reminder, the whole motor network ROI was defined using an ICA spatial map representing the motor network.

In the M1 group, MEP change did not correlate with either initial rs-fMRI FC between left M1 and the whole motor network (n = 13, r = 0.48, $P_{uncorr} = 0.09$, $P_{corr} = 0.36$), initial MSE in left M1 (n = 13, r = 0.18, $P_{uncorr} = 0.56$, $P_{corr} > 0.9$), FA in the left M1 tract (n = 13, r = 0.29, $P_{uncorr} = 0.38$, $P_{corr} > 0.9$), or cortical thickness in left M1 (n = 13, r =-0.25, $P_{uncorr} = 0.39$, $P_{corr} > 0.9$).

In the PMd group, MEP change showed a positive correlation with the FA in the left PMd tract (n = 15, r = 0.62, t(13) = 2.89, $P_{uncorr} = 0.012$, $P_{corr} = 0.048$), but it did not correlate with the initial resting-state functional connectivity between the left PMd and the whole motor network (n = 15, r = -0.02, $P_{uncorr} = 0.9$, $P_{corr} > 0.9$), initial MSE in left PMd (n = 15, r = 0.19, $P_{uncorr} = 0.49$, $P_{corr} > 0.9$), or cortical thickness in left PMd (n = 15, r =-0.13, $P_{uncorr} = 0.65$, $P_{corr} > 0.9$).

Differences between responders and non-responders

To evaluate whether any of the above factors could explain the distinction between responders and non-responders, we compared the factors listed above (initial rs-fMRI FC, initial MSE, FA, and cortical thickness) between responders and non-responders in the M1 and PMd groups. As a reminder, in the M1 group, there were 6 responders and 7 non-responders; in the PMd group, there were 11 responders and 4 non-responders. These are small sample sizes and thus provide only an exploratory look at differences between responders and non-responders.

In the M1 group, there were no significant differences between responders and non-responders in any of the factors: initial rs-fMRI FC between left M1 and the whole motor network (responders: 0.82 ± 0.23, non-responders: 0.59 ± 0.21, t(10.26) = 1.85, n = 13, $P_{uncorr} = 0.09$, $P_{corr} = 0.36$), initial MSE in left M1 (responders:0.94 ± 0.08, non-responders: 0.87 ± 0.07, t(10.27) = 1.61, n = 13, $P_{uncorr} = 0.14$, $P_{corr} = 0.56$), FA of the left M1 tract (responders: 0.55 ± 0.01, non-responders: 0.54 ± 0.02, t(8.921) = 0.69, n = 13, $P_{uncorr} = 0.51$, $P_{corr} > 0.9$), or cortical thickness of left M1

(responders: 2.22 ± 0.23, non-responders: 2.17 ± 0.09, t(9.361) = 0.46, n = 13, P_{uncorr} = 0.66, $P_{corr} > 0.9$).

In the PMd group, only the FA in the left PMd tract was higher in responders (0.55 ± 0.01) compared to non-responders (0.52 ± 0.003; t(12.73) = 6.09, n = 15, $P_{uncorr} < 0.001$, $P_{corr} < 0.001$). For all the other measurements, there were no significant differences between responders and non-responders: initial resting-state functional connectivity between left PMd and the whole motor network (responders: -0.08 ± 0.35, non-responders: 0.10 ± 0.25, t(7.796) =1.08, n = 15, $P_{uncorr} = 0.31$, $P_{corr} > 0.9$), initial MSE in left PMd (responders: 0.78 ± 0.08, non-responders: 0.75 ± 0.07 , t(5.793) = 0.70, n = 15, P_{uncorr} = 0.51, $P_{corr} > 0.9$), or the cortical thickness of left PMd (responders: 2.84 ± 0.21, non-responders: 2.88 ± 0.38, t(3.651) = 0.20, n = 15, $P_{uncorr} = 0.85$, $P_{corr} > 0.9$).

Comparison of the stimulation site localization

Finally, as we collected both TMS and MRI with tDCS stimulation sites localized on them, we performed a post-hoc analysis to examine if the individual locations of M1 and PMd, defined using standard TMS and tDCS brain stimulation protocols, matched the functional/anatomical definitions for these regions on their MRIs. We used the same ROIs from the Hardwick meta-analysis[19] to define the standard functional M1 and PMd locations (see Figure 2). The standard functional M1 location matched the hand knob[44], which is commonly thought to represent the anatomical location of the motor hand area. For PMd, due to the large extent of the anatomical PMd, the standard functional PMd was within its anatomical extent. To note, however, some studies found activation associated with motor performance and motor learning in a more anterior part of the anatomical PMd boundaries[45] compared to Hardwick location[19]. We quantified the distance of each

individual's stimulated region from the standard M1/PMd ROIs by computing the minimum Hausdorff's distance (i.e., the minimum distance between the two ROI boundaries)[46].

In the M1 group, the average Hausdorff's distance between the individual stimulation site and the standard M1 was 3.79±4.64mm, and with the standard PMd, it was 3.46±4.89mm. In the PMd group, the average Hausdorff's distance between the individual stimulation site and the standard PMd was 4.93±4.80mm, and with the standard M1, it was 15.44±4.78mm.

In terms of the number of individuals with overlap with each ROI, in the M1 group, the M1 stimulation site overlapped with the standard M1 ROI in 6 participants and with the standard PMd ROI in 6 participants. In the remaining 3 participants, the stimulation site was localized between the M1 and PMd ROIs. In the PMd group, the PMd stimulation site overlapped with the standard PMd ROI in 5 participants and with the standard M1 ROI in 2 participants. In the other 8 participants, the stimulation site localization was localized a little anteriorly to the standard PMd ROI, but still within the anatomical (atlas-based) extent of PMd.

Finally, Pearson correlations between the distance from each ROI and MEP changes showed only a non-significant trend for each group. In the M1 group, participants with the greatest MEP changes also tended to have the largest distance between the stimulation site and the PMd ROI ($t(13) = 2.3$, $n = 15$, $r = 0.53$, $P = 0.06$). In contrast, in the PMd group, participants with the greatest MEP changes also tended to have the shortest distance between the stimulation site and the PMd ROI ($t(13) = 1.8$, $n = 15$, $r = -0.48$, $P = 0.07$). There were no significant correlations between these distances and changes in MSE post-HD-tDCS in any group. To see a visualization of the overlap of each individual stimulation site with the standard ROIs, see Figure 7. For more information and correlation plots, see *Supplementary Figure 3*.

Overall, this suggests that there is large inter-individual variability in M1 and PMd localization using canonical methods (e.g., defining M1 as the TMS motor hotspot and PMd as 2.5 cm anterior to the motor hotspot). In particular, many individuals in the M1 group had M1 stimulation sites that were bordering or overlapping with PMd. This heterogeneity in stimulation site may have contributed the variability of responsiveness to HD-tDCS.

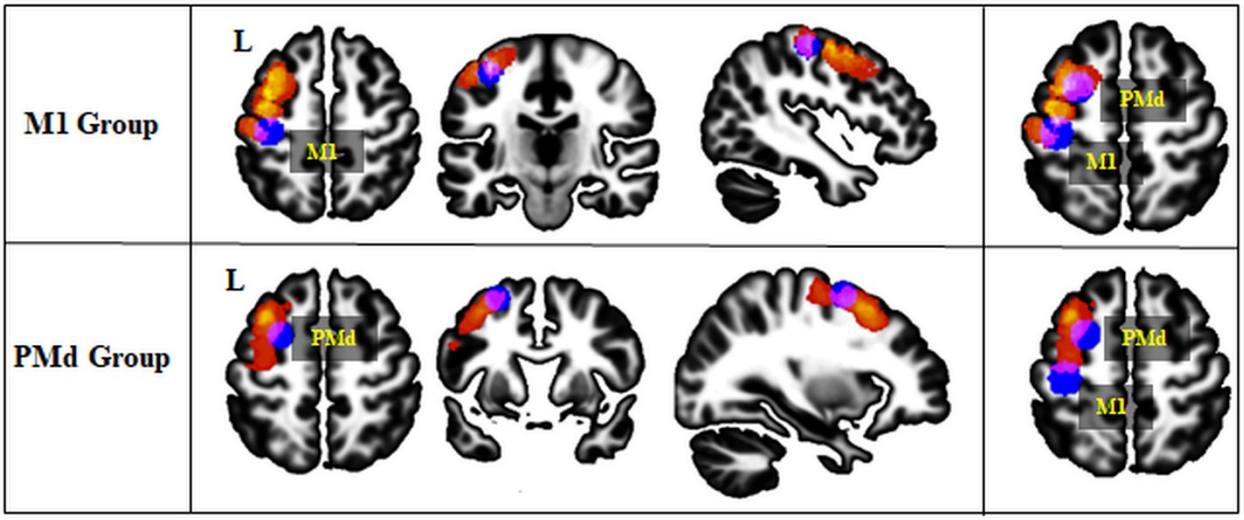

Figure 7: Localization of the stimulation site. This figure displays the localization of the actual stimulation sites in all the participants and shows an overlap of these sites with the standard left M1 or left PMd localization for both groups. The actual stimulation sites are presented in a heat map, with individual subjects plotted in red and overlap between participants reflected in warmer colors (with yellow representing the surface shared by most of the participants). The standard M1 and PMd ROIs are displayed in blue. The overlap between the actual and standard localization is colored in purple. *M1: primary motor area, PMd: dorsal premotor cortex, L: left.*

DISCUSSION

In this study, we performed a systematic, double-blind investigation using concurrent HD-tDCS and fMRI to examine changes in brain excitability, network connectivity and complexity before and after HD-tDCS stimulation of either M1 or PMd. To our knowledge, this is the first known group study using concurrent HD-tDCS and fMRI, although a previous pilot study examined the safety of a similar protocol in one single participant[30]. In addition to concurrent HD-tDCS and fMRI, we also examined changes in cortical excitability using TMS before and after HD-tDCS. We also investigated whether any baseline measures of cortical connectivity, complexity or neuroanatomy correlated with response to HD-tDCS in either group. Finally, we explored the interindividual variability in stimulation site using canonical localization techniques, and reported the distance between actual versus expected stimulation sites.

Overall, we found that HD-tDCS over left PMD produced more slightly reliable increases in cortical excitability than HD-tDCS over left M1 or sham. In addition, this increase of cortical excitability in the PMd group was accompanied by modulations in motor network complexity, observed only after PMd HD-tDCS and not after M1 HD-tDCS. Furthermore, the strength of the CST originating from left PMd demonstrated a significant positive correlation with the magnitude MEP change following HD-tDCS over PMd and was significantly different between responders versus non-responders in the PMd group. No other functional or structural markers correlated with MEP response in the PMd group, and no markers at all were correlated with MEP response in the M1 group. Finally, we showed that there was significant variability in the location of the actual stimulation sites compared to the expected stimulation sites based on canonical electrode placement – a factor which may introduce additional variability into studies of brain stimulation.

PMd HD-tDCS leads to more reliable changes in cortical excitability than M1 HD-tDCS

As we hypothesized, we observed that PMd-HD-tDCS induced a slightly more reliable increase of MEPs, resulting in 75% responders (i.e., participants who demonstrated an increase in MEP amplitude after HD-tDCS) compared to only 50% responders in the M1 group. However, when examining just the participants who responded to the stimulation, both M1 and PMd HD-tDCS led to significant increases in MEP amplitude after HD-tDCS, with no significant differences in amplitude between the groups. This suggests that changing the entry point into the motor network from M1 to PMd increases the reliability of HD-tDCS effects on cortical excitability but not the amplitude of changes in the responders. Similar to what has been previously suggested[5], here we showed that M1-HD-tDCS may not be the best target to consistently enhance cortical excitability, even in healthy volunteers. Moreover, in line with recent studies from stroke rehabilitation, targeting PMd may be an effective option to enhance the excitability of the motor network[47]. This study used a modest sample of 15-16 participants per group and had relatively modest effect sizes; future studies with more participants are needed to confirm this finding.

Network changes following HD-tDCS

Functional connectivity

Both M1 and PMd HD-tDCS led to no differences in motor network FC. Although previous work has suggested that tDCS may induce changes in FC of the motor network[48,49], our analyses showed no significant changes. Our exploratory analyses, at a lower threshold, presented in *Supplementary Data 2 and 3, Supplementary Figures 1 and 2, and Supplementary Discussion*, demonstrated some trends towards modifications in FC occurred after HD-tDCS but these modifications are only significant at lower thresholds. It is possible that the short duration of the HD-tDCS session (7 minutes) and low amplitude of current (1 mA) might not have been sufficient

to induce reliable and significantly different changes in the FC of the motor network, which had been previously observed after 10 to 20 minutes of stimulation[48,49].

Multiscale Entropy

MSE, a method for measuring the complexity of finite length time series, quantifies the regularity of a time series by calculating the complexity of a signal at different time scales[50]. This measure is used as a complexity measure for neuroimaging signals[51-53] and reflects the dynamics of the neural networks[27]. Previous work has shown that increasing brain complexity is associated with brain adaptation[25,26]. Importantly, MSE is thought to measure fine-grained changes in brain function following tDCS[25,28,54]. As hypothesized, PMd HD-tDCS also led to significant and more reliable changes in MSE than M1 HD-tDCS (i.e., a strong increase of the MSE in the left PMd along with a decrease of the MSE in the right PMd). On the other hand, no significant MSE changes were observed after M1 HD-tDCS. Given that PMd HD-tDCS led to more reliable changes in cortical excitability, it is likely this was also captured in the MSE changes found in both hemisphere (i..e., an enhancement of the excitability in the stimulated hemisphere associated with a decrease of the excitability in the second hemisphere[55,56]). In line with previous studies[26], MSE and FC seemed to be complementary metrics: MSE may be more sensitive and able to capture changes in a node of the motor network whereas traditional rs-fMRI FC would capture changes between nodes.

Fractional anisotropy of the corticospinal tract corresponds to HD-tDCS response in the PMd group

Previous research has shown difficulty finding reliable biomarkers that predict responsiveness to HD-tDCS. Examples of proposed but variable biomarkers include neurochemical or genetic

variants[57-59] and EEG-based measures of brain activity[60]. However, recent studies have suggested that functional connectivity[61], as well as the integrity of the white matter fiber tracts originating from the targeted area[62], could predict the response to HD-tDCS. In the present study, none of the measured parameters tended to correlate with the change in MEP amplitude after M1 HD-tDCS. On the other hand, in the PMd group, similar to what was observed previously[62], higher FA in the part of the CST that originated from left PMd was related to increased MEP amplitude after PMd HD-tDCS. Moreover, stronger FA values in the left PMd-portion of the CST were observed in the participants who responded to PMd HD-tDCS. This suggests that the strength of the corticospinal tract originating from PMd may be a predictor of HD-tDCS response in some participants and should be further examined.

Wide inter-individual variability is observed after tDCS

In the present study, we observed high inter-individual variability in HD-tDCS-induced changes in cortical excitability. This variability is similar to what has been recently reported, with up to 50% of participants showing no response to tDCS[4,63,64]. However, changing the neural target from M1 to PMd enhanced the reliability of the response to HD-tDCS. That is, the variability associated with HD-tDCS was reduced in the PMd-HD-tDCS group and changes in MSE were detected following PMd HD-tDCS, although not M1 HD-tDCS. This suggests that stimulating PMd to modulate the motor network might help reduce interindividual variability compared to stimulating M1.

In addition to the choice of the stimulation target, the position of the electrodes may also introduce considerable variability. In accordance with the canonical methods for electrode placement, we localized M1 based on the motor hotspot and PMd 2.5 centimeters anterior to the motor hotspot[47]. As displayed in Figure 7, despite using this established localization method, the

position of the stimulated area was highly variable across individuals when compared with their expected anatomical location. Specifically, in the M1 group, in more than half of the participants, the actual localization of the stimulation did not overlap with the standard M1 localization[19]. In contrast, as the PMd was slightly wider, more individuals fell within the PMd ROI definition or within its anatomical boundaries (slightly anterior to the PMd ROI). Therefore, it seems that the one-size-fits-all method to localize the target area may not be effective in everyone. It also suggests that the motor hotspot may not always be localized at M1, but may bleed into the adjacent premotor cortex, as previously observed[65]. This is likely due to differences in brain structure between individuals[66]. Moreover, some studies with primates showed both M1 and the adjacent PMd were involved in maps of motor control, without any clear functional boundaries between the regions[67-69]. This suggests that the motor hotspot localization using TMS cannot be assumed to be M1 (hand knob) but may also be a location within the premotor cortex. Similarly, since the PMd localization is dependent on the location of the motor hotspot, this leads to variation in PMd as well. In our study, the actual PMd stimulation location did not always overlap with the functional PMd localization (as obtained from the Hardwick meta-analysis[19]) but it still overlapped with the anatomical PMd boundaries. In future work, if it is possible to first obtain an MRI, it may be advisable to use neuroanatomical constraints on the motor hotspot localization using the individual's MRI and neuronavigation-guided TMS to find the spot within the anatomical area that provides the strongest response. This might help to reduce inter-individual variability in experimental parameters. In the practical constraint that an MRI cannot be obtained prior to TMS, registering all participants to a template brain to guide and record motor hotspot localization may be an alternative solution.

Limitations

The present study has several limitations. First, although the size of our groups (n=15-16 per group) is larger than recent studies exploring significant changes in cortical excitability following brain stimulation, these groups are still relatively small, especially given the large variability within each group. Second, in the present study, we used a short 7-minute stimulation duration at 1 mA current, which may not have been sufficient to induce a strong effect in cortical excitability or network changes. However, this study demonstrated that stimulating a brain region other than M1 (in this case, PMd) even for a short period can lead to a strong and reliable enhancement of cortical excitability, suggesting it was strong enough to elicit some changes. However, future work may examine whole-brain network changes following longer durations or higher intensities of HD-tDCS. Third, we used a parallel study design, as opposed to a cross-over design. Each participant received HD-tDCS over only one neural target (M1 or PMd). Consequently, we cannot affirm that the participants who responded to PMd HD-tDCS would have not also have responded to M1 HD-tDCS, or vice-versa. Future studies involving a larger sample size and a cross-over design are needed to answer this specific question.

Conclusion

To our knowledge, this is the first large study employing HD-tDCS with fMRI in a double-blind design with multiple stimulation sites. Using this design, we investigated the neurophysiological effects of tDCS on the motor network immediately after stimulation. We compared HD-tDCS over M1 versus PMd, and showed that PMd HD-tDCS may modulate motor network excitability and neural complexity more robustly than M1 HD-tDCS. These results also suggest that multiscale entropy may be a sensitive measure of changes in neuronal excitability

following noninvasive brain stimulation within a single region, and may be able to detect changes not detected by more standard functional connectivity measures. We further showed that response to PMd HD-tDCS may be predicted by the integrity of the cortical spinal tract originating from PMd. Finally, we demonstrate that conventional methods for defining tDCS targets such as M1 and PMd may be influenced by large inter-individual variability in the motor hotspot location. Future work should carefully consider and account for the actual, versus assumed, stimulated location. Altogether, these results open new considerations for improving the efficacy of tDCS on modulating the motor network.

Data availability

The unthresholded statistical maps used to generate the motor network (i.e., ICA analyses) are stored on the NEUROVAULT repository (https://neurovault.org/collections/UTZRKARR/). The individual MEPs, MSE and FA data for each participant are stored on the OSF repository (https://osf.io/m94c6/?view_only=093167bbffa148f7b4b0540315cff5bd). The raw data supporting these analyses will be made available following reasonable requests to the corresponding author. These data are not publicly available due to IRB restrictions.

Acknowledgments

We would like to thank all the study participants, as well as Katherin Martin for her help during the MRI acquisition. We also acknowledge our funding sources, including several NIH grants that supported this work (NIH K01HD091283, R61MH110526 and R01MH111896) and the USC Provost's Postdoctoral Scholar Research Grant.

Author contributions

S-L L and S.L. conceived and designed the study with input from D.J.J.W., K.J., and N.S.,
S.L., M.J. K.I., A.S. acquired the data,
S.L. M.J., K.J., Y.Q., R.C., Y.S., and S.L.L. contributed to the data analyses and interpretation,
S.L. and S-L.L. wrote the paper with contributions from all the authors,
All the authors agreed with the submitted version or the paper.

Competing interests

The authors declare no competing interests.

Corresponding author:

Correspondence to Sook-Lei Liew

REFERENCES

1 Nitsche, M. A. & Paulus, W. Excitability changes induced in the human motor cortex by weak transcranial direct current stimulation. *J Physiol.* (2000) **527 Pt 3**, 633-639.

2 Lefebvre, S. & Liew, S. L. Anatomical Parameters of tDCS to Modulate the Motor System after Stroke: A Review. *Front Neurol.* (2017) **8**, 29.

3 Shaheiwola, N., Zhang, B., Jia, J. & Zhang, D. Using tDCS as an Add-On Treatment Prior to FES Therapy in Improving Upper Limb Function in Severe Chronic Stroke Patients: A Randomized Controlled Study. *Front Hum Neurosci.* (2018) **12**, 233.

4 Ammann, C., Lindquist, M. A. & Celnik, P. A. Response variability of different anodal transcranial direct current stimulation intensities across multiple sessions. *Brain Stimul.* (2017) **10**, 757-763.

5 Lopez-Alonso, V., Liew, S. L., Fernandez Del Olmo, M., Cheeran, B., Sandrini, M., Abe, M. & Cohen, L. G. A Preliminary Comparison of Motor Learning Across Different Non-invasive Brain Stimulation Paradigms Shows No Consistent Modulations. *Front Neurosci.* (2018) **12**, 253.

6 Dum, R. P. & Strick, P. L. The origin of corticospinal projections from the premotor areas in the frontal lobe. *J Neurosci.* (1991) **11**, 667-689.

7 Barbas, H. & Pandya, D. N. Architecture and frontal cortical connections of the premotor cortex (area 6) in the rhesus monkey. *J Comp Neurol.* (1987) **256**, 211-228.

8 Kantak, S. S., Stinear, J. W., Buch, E. R. & Cohen, L. G. Rewiring the brain: potential role of the premotor cortex in motor control, learning, and recovery of function following brain injury. *Neurorehabilitation and neural repair.* (2012) **26**, 282-292.

9 Etkin, A., Egner, T. & Kalisch, R. Emotional processing in anterior cingulate and medial prefrontal cortex. *Trends in cognitive sciences.* (2011) **15**, 85-93.

10 Fujiyama, H., Hinder, M. R. & Summers, J. J. Functional role of left PMd and left M1 during preparation and execution of left hand movements in older adults. *J Neurophysiol.* (2013) **110**, 1062-1069.

11 Thura, D. & Cisek, P. Deliberation and commitment in the premotor and primary motor cortex during dynamic decision making. *Neuron.* (2014) **81**, 1401-1416.

12 Dum, R. P. & Strick, P. L. Frontal lobe inputs to the digit representations of the motor areas on the lateral surface of the hemisphere. *J Neurosci.* (2005) **25**, 1375-1386.

13 Burman, K. J., Bakola, S., Richardson, K. E., Reser, D. H. & Rosa, M. G. Patterns of cortical input to the primary motor area in the marmoset monkey. *J Comp Neurol.* (2014) **522**, 811-843.

14 Bestmann, S. & Krakauer, J. W. The uses and interpretations of the motor-evoked potential for understanding behaviour. *Exp Brain Res.* (2015) **233**, 679-689.

15 Wymbs, N. F. & Grafton, S. T. Contributions from the left PMd and the SMA during sequence retrieval as determined by depth of training. *Exp Brain Res.* (2013) **224**, 49-58.

16 Neva, J. L., Vesia, M., Singh, A. M. & Staines, W. R. Modulation of left primary motor cortex excitability after bimanual training and intermittent theta burst stimulation to left dorsal premotor cortex. *Behav Brain Res.* (2014) **261**, 289-296.

17 Stinear, C. M., Barber, P. A., Coxon, J. P., Verryt, T. S., Acharya, P. P. & Byblow, W. D. Repetitive stimulation of premotor cortex affects primary motor cortex excitability and movement preparation. *Brain Stimul.* (2009) **2**, 152-162.

18 Umilta, M. A., Brochier, T., Spinks, R. L. & Lemon, R. N. Simultaneous recording of macaque premotor and primary motor cortex neuronal populations reveals different functional contributions to visuomotor grasp. *J Neurophysiol.* (2007) **98**, 488-501.

19 Hardwick, R. M., Rottschy, C., Miall, R. C. & Eickhoff, S. B. A quantitative meta-analysis and review of motor learning in the human brain. *Neuroimage.* (2013) **67**, 283-297.

20 Buch, E. R., Santarnecchi, E., Antal, A., Born, J., Celnik, P. A., Classen, J. *et al.* Effects of tDCS on motor learning and memory formation: A consensus and critical position paper. *Clin Neurophysiol.* (2017) **128**, 589-603.

21 Nitsche, M. A., Doemkes, S., Karakose, T., Antal, A., Liebetanz, D., Lang, N., Tergau, F. & Paulus, W. Shaping the effects of transcranial direct current stimulation of the human motor cortex. *J Neurophysiol.* (2007) **97**, 3109-3117.

22 Kuo, H. I., Bikson, M., Datta, A., Minhas, P., Paulus, W., Kuo, M. F. & Nitsche, M. A. Comparing cortical plasticity induced by conventional and high-definition 4 x 1 ring tDCS: a neurophysiological study. *Brain Stimul.* (2013) **6**, 644-648.

23 Caparelli-Daquer, E. M., Zimmermann, T. J., Mooshagian, E., Parra, L. C., Rice, J. K., Datta, A., Bikson, M. & Wassermann, E. M. A pilot study on effects of 4x1 high-definition tDCS on motor cortex excitability. *Conf Proc IEEE Eng Med Biol Soc.* (2012) **2012**, 735-738.

24 Lefebvre, S., Dricot, L., Laloux, P., Desfontaines, P., Evrard, F., Peeters, A., Jamart, J. & Vandermeeren, Y. Increased functional connectivity one week after motor learning and tDCS in stroke patients. *Neuroscience.* (2017) **340**, 424-435.

25 Liang, W. K., Lo, M. T., Yang, A. C., Peng, C. K., Cheng, S. K., Tseng, P. & Juan, C. H. Revealing the brain's adaptability and the transcranial direct current stimulation facilitating effect in inhibitory control by multiscale entropy. *Neuroimage.* (2014) **90**, 218-234.

26 Wang, D. J. J., Jann, K., Fan, C., Qiao, Y., Zang, Y. F., Lu, H. & Yang, Y. Neurophysiological Basis of Multi-Scale Entropy of Brain Complexity and Its Relationship With Functional Connectivity. *Front Neurosci.* (2018) **12**, 352.

27 Heisz, J. J., Shedden, J. M. & McIntosh, A. R. Relating brain signal variability to knowledge representation. *Neuroimage.* (2012) **63**, 1384-1392.

28 Kang, J., Cai, E., Han, J., Tong, Z., Li, X., Sokhadze, E. M., Casanova, M. F. & Ouyang, G. Transcranial Direct Current Stimulation (tDCS) Can Modulate EEG Complexity of Children With Autism Spectrum Disorder. *Front Neurosci.* (2018) **12**, 201.

29 Giordano, J., Bikson, M., Kappenman, E. S., Clark, V. P., Coslett, H. B., Hamblin, M. R. *et al.* Mechanisms and Effects of Transcranial Direct Current Stimulation. *Dose Response.* (2017) **15**, 1559325816685467.

30 Gbadeyan, O., Steinhauser, M., McMahon, K. & Meinzer, M. Safety, Tolerability, Blinding Efficacy and Behavioural Effects of a Novel MRI-Compatible, High-Definition tDCS Set-Up. *Brain stimulation.* (2016) **9**, 545-552.

31 Schambra, H. M., Ogden, R. T., Martinez-Hernandez, I. E., Lin, X., Chang, Y. B., Rahman, A., Edwards, D. J. & Krakauer, J. W. The reliability of repeated TMS measures in older adults and in patients with subacute and chronic stroke. *Front Cell Neurosci.* (2015) **9**, 335.

32 Wagle-Shukla, A., Ni, Z., Gunraj, C. A., Bahl, N. & Chen, R. Effects of short interval intracortical inhibition and intracortical facilitation on short interval intracortical facilitation in human primary motor cortex. *J Physiol.* (2009) **587**, 5665-5678.

33 Rizzo, V., Siebner, H. R., Modugno, N., Pesenti, A., Munchau, A., Gerschlager, W., Webb, R. M. & Rothwell, J. C. Shaping the excitability of human motor cortex with premotor rTMS. *J Physiol.* (2004) **554**, 483-495.

34 Whitfield-Gabrieli, S. & Nieto-Castanon, A. Conn: a functional connectivity toolbox for correlated and anticorrelated brain networks. *Brain Connect.* (2012) **2**, 125-141.

35 McDonough, I. M. & Nashiro, K. Network complexity as a measure of information processing across resting-state networks: evidence from the Human Connectome Project. *Frontiers in human neuroscience.* (2014) **8**, 409-409.

36 Yang, A. C., Tsai, S. J., Lin, C. P. & Peng, C. K. A Strategy to Reduce Bias of Entropy Estimates in Resting-State fMRI Signals. *Frontiers in neuroscience.* (2018) **12**, 398.

37 Shi, Y. & Toga, A. W. Connectome imaging for mapping human brain pathways. *Mol Psychiatry.* (2017) **22**, 1230-1240.

38 Cabeen, R. P., Bastin, M. E. & Laidlaw, D. H. Kernel regression estimation of fiber orientation mixtures in diffusion MRI. *Neuroimage.* (2016) **127**, 158-172.

39 Cabeen RP, Laidlaw DH & AW, T. *Quantitative Imaging Toolkit: Software for Interactive 3D Visualization, Data Exploration, and Computational Analysis of Neuroimaging Datasets*. *Proc International Society for Magnetic Resonance in Medicine (ISMRM)* (2018), 2854.

40 Archer, D. B., Vaillancourt, D. E. & Coombes, S. A. A Template and Probabilistic Atlas of the Human Sensorimotor Tracts using Diffusion MRI. *Cereb Cortex.* (2018) **28**, 1685-1699.

41 Fischl, B. & Dale, A. M. Measuring the thickness of the human cerebral cortex from magnetic resonance images. *Proc Natl Acad Sci U S A.* (2000) **97**, 11050-11055.

42 Guerra, A., Lopez-Alonso, V., Cheeran, B. & Suppa, A. Solutions for managing variability in non-invasive brain stimulation studies. *Neurosci Lett.* (2017).

43 Diedenhofen, B. & Musch, J. cocor: a comprehensive solution for the statistical comparison of correlations. *PLoS One.* (2015) **10**, e0121945.

44 Yousry, T. A., Schmid, U. D., Alkadhi, H., Schmidt, D., Peraud, A., Buettner, A. & Winkler, P. Localization of the motor hand area to a knob on the precentral gyrus. A new landmark. *Brain.* (1997) **120 (Pt 1)**, 141-157.

45 Mayka, M. A., Corcos, D. M., Leurgans, S. E. & Vaillancourt, D. E. Three-dimensional locations and boundaries of motor and premotor cortices as defined by functional brain imaging: a meta-analysis. *Neuroimage.* (2006) **31**, 1453-1474.

46 Fedorov, A., Billet, E., Prastawa, M., Gerig, G., Radamanesh, A., Warfield, S., K.,, Kikinis, R. & Chrisochoides, N. in *Advances in Visual Computing. ISVC 2008. Lecture Notes in Computer Science* Vol. 5358 (ed Bebis G. et al. (eds)) (Springer, Berlin, Heidelberg, 2008).

47 Cunningham, D. A., Varnerin, N., Machado, A., Bonnett, C., Janini, D., Roelle, S., Potter-Baker, K., Sankarasubramanian, V., Wang, X., Yue, G. & Plow, E. B. Stimulation targeting higher motor areas in stroke rehabilitation: A proof-of-concept, randomized, double-blinded placebo-controlled study of effectiveness and underlying mechanisms. *Restor Neurol Neurosci.* (2015) **33**, 911-926.

48 Amadi, U., Ilie, A., Johansen-Berg, H. & Stagg, C. J. Polarity-specific effects of motor transcranial direct current stimulation on fMRI resting state networks. *Neuroimage.* (2014) **88**, 155-161.

49 Sehm, B., Kipping, J., Schafer, A., Villringer, A. & Ragert, P. A Comparison between Uni- and Bilateral tDCS Effects on Functional Connectivity of the Human Motor Cortex. *Front Hum Neurosci.* (2013) **7**, 183.

50 Costa, M., Goldberger, A. L. & Peng, C. K. Multiscale entropy analysis of biological signals. *Phys Rev E Stat Nonlin Soft Matter Phys.* (2005) **71**, 021906.

51 Li, X., Zhu, Z., Zhao, W., Sun, Y., Wen, D., Xie, Y., Liu, X., Niu, H. & Han, Y. Decreased resting-state brain signal complexity in patients with mild cognitive impairment and Alzheimer's disease: a multiscale entropy analysis. *Biomed Opt Express.* (2018) **9**, 1916-1929.

52 McDonough, I. M. & Nashiro, K. Network complexity as a measure of information processing across resting-state networks: evidence from the Human Connectome Project. *Front Hum Neurosci.* (2014) **8**, 409.

53 Smith, R. X., Yan, L. & Wang, D. J. Multiple time scale complexity analysis of resting state FMRI. *Brain Imaging and Behavior.* (2014) **8**, 284-291.

54 Lafontaine, M. P., Lacourse, K., Lina, J. M., McIntosh, A. R., Gosselin, F., Theoret, H. & Lippe, S. Brain signal complexity rises with repetition suppression in visual learning. *Neuroscience.* (2016) **326**, 1-9.

55 Shin, S. S. & Pelled, G. Novel Neuromodulation Techniques to Assess Interhemispheric Communication in Neural Injury and Neurodegenerative Diseases. *Front Neural Circuits.* (2017) **11**, 15.

56 Mondini, V., Mangia, A. L. & Cappello, A. Single-session tDCS over the dominant hemisphere affects contralateral spectral EEG power, but does not enhance neurofeedback-guided event-related desynchronization of the non-dominant hemisphere's sensorimotor rhythm. *PLoS One.* (2018) **13**, e0193004.

57 Antal, A., Chaieb, L., Moliadze, V., Monte-Silva, K., Poreisz, C., Thirugnanasambandam, N., Nitsche, M. A., Shoukier, M., Ludwig, H. & Paulus, W. Brain-derived neurotrophic factor (BDNF) gene polymorphisms shape cortical plasticity in humans. *Brain Stimul.* (2010) **3**, 230-237.

58 Brunoni, A. R., Kemp, A. H., Shiozawa, P., Cordeiro, Q., Valiengo, L. C., Goulart, A. C. *et al.* Impact of 5-HTTLPR and BDNF polymorphisms on response to sertraline versus transcranial direct current stimulation: implications for the serotonergic system. *Eur Neuropsychopharmacol.* (2013) **23**, 1530-1540.

59 Puri, R., Hinder, M. R. & Summers, J. J. The BDNF Val66Met polymorphism modulates motor cortex plasticity, induced by prolonged anodal transcranial direct current stimulation, in older adults. *Brain Stimulation: Basic, Translational, and Clinical Research in Neuromodulation.* (2015) **8**, 336.

60 Nuzum, N. D., Hendy, A. M., Russell, A. P. & Teo, W. P. Measures to Predict The Individual Variability of Corticospinal Responses Following Transcranial Direct Current Stimulation. *Front Hum Neurosci.* (2016) **10**, 487.

61 Hordacre, B., Moezzi, B., Goldsworthy, M. R., Rogasch, N. C., Graetz, L. J. & Ridding, M. C. Resting state functional connectivity measures correlate with the response to anodal transcranial direct current stimulation. *Eur J Neurosci.* (2017) **45**, 837-845.

62 Lin, R. L., Douaud, G., Filippini, N., Okell, T. W., Stagg, C. J. & Tracey, I. Structural Connectivity Variances Underlie Functional and Behavioral Changes During Pain Relief Induced by Neuromodulation. *Sci Rep.* (2017) **7**, 41603.

63 Wiethoff, S., Hamada, M. & Rothwell, J. C. Variability in response to transcranial direct current stimulation of the motor cortex. *Brain Stimul.* (2014) **7**, 468-475.

64 Lopez-Alonso, V., Fernandez-Del-Olmo, M., Costantini, A., Gonzalez-Henriquez, J. J. & Cheeran, B. Intra-individual variability in the response to anodal transcranial direct current stimulation. *Clin Neurophysiol.* (2015) **126**, 2342-2347.

65 Ahdab, R., Ayache, S. S., Brugieres, P., Farhat, W. H. & Lefaucheur, J. P. The Hand Motor Hotspot is not Always Located in the Hand Knob: A Neuronavigated Transcranial Magnetic Stimulation Study. *Brain Topogr.* (2016) **29**, 590-597.

66 Valizadeh, S. A., Liem, F., Merillat, S., Hanggi, J. & Jancke, L. Identification of individual subjects on the basis of their brain anatomical features. *Sci Rep.* (2018) **8**, 5611.

67 Godschalk, M., Mitz, A. R., van Duin, B. & van der Burg, H. Somatotopy of monkey premotor cortex examined with microstimulation. *Neurosci Res.* (1995) **23**, 269-279.

68 Graziano, M. S., Taylor, C. S. & Moore, T. Complex movements evoked by microstimulation of precentral cortex. *Neuron.* (2002) **34**, 841-851.

69 Graziano, M. S., Taylor, C. S., Moore, T. & Cooke, D. F. The cortical control of movement revisited. *Neuron.* (2002) **36**, 349-362.